Circulation
JOURNAL OF THE AMERICAN HEART ASSOCIATION

American Heart Association®

Macrophage Gene Expression and Foam Cell Formation Are Regulated by Plasminogen

Riku Das, Swetha Ganapathy, Ganapati H. Mahabeleshwar, Carla Drumm, Maria Febbraio, Mukesh K. Jain and Edward F. Plow

Circulation. 2013;127:1209-1218; originally published online February 11, 2013;
doi: 10.1161/CIRCULATIONAHA.112.001214
Circulation is published by the American Heart Association, 7272 Greenville Avenue, Dallas, TX 75231
Copyright © 2013 American Heart Association, Inc. All rights reserved.
Print ISSN: 0009-7322. Online ISSN: 1524-4539

The online version of this article, along with updated information and services, is located on the World Wide Web at:
http://circ.ahajournals.org/content/127/11/1209

An erratum has been published regarding this article. Please see the attached page for:
http://circ.ahajournals.org/content/129/5/e326.full.pdf

Data Supplement (unedited) at:
http://circ.ahajournals.org/content/suppl/2013/02/11/CIRCULATIONAHA.112.001214.DC1.html

Permissions: Requests for permissions to reproduce figures, tables, or portions of articles originally published in *Circulation* can be obtained via RightsLink, a service of the Copyright Clearance Center, not the Editorial Office. Once the online version of the published article for which permission is being requested is located, click Request Permissions in the middle column of the Web page under Services. Further information about this process is available in the Permissions and Rights Question and Answer document.

Reprints: Information about reprints can be found online at:
http://www.lww.com/reprints

Subscriptions: Information about subscribing to *Circulation* is online at:
http://circ.ahajournals.org//subscriptions/

Downloaded from http://circ.ahajournals.org/ at INSERM U460 UFR XAVIER BI on March 3, 2014

Macrophage Gene Expression and Foam Cell Formation Are Regulated by Plasminogen

Riku Das, PhD; Swetha Ganapathy, MS*; Ganapati H. Mahabeleshwar, PhD*; Carla Drumm, BS; Maria Febbraio, PhD; Mukesh K. Jain, MD; Edward F. Plow, PhD

Background—Deciphering the molecular and cellular processes that govern macrophage foam cell formation is critical to understanding the basic mechanisms underlying atherosclerosis and other vascular pathologies.

Methods and Results—Here, we identify a pivotal role of plasminogen (Plg) in regulating foam cell formation. Deficiency of Plg inhibited macrophage cholesterol accumulation on exposure to hyperlipidemic conditions in vitro, ex vivo, and in vivo. Gene expression analysis identified CD36 as a regulated target of Plg, and macrophages from $Plg^{-/-}$ mice had decreased CD36 expression and diminished foam cell formation. The Plg-dependent CD36 expression and foam cell formation depended on conversion of Plg to plasmin, binding to the macrophage surface, and the consequent intracellular signaling that leads to production of leukotriene B_4. Leukotriene B_4 rescued the suppression of CD36 expression and foam cell formation arising from Plg deficiency.

Conclusions—Our findings demonstrate an unanticipated role of Plg in the regulation of gene expression and cholesterol metabolism by macrophages and identify Plg-mediated regulation of leukotriene B^4 as an underlying mechanism. **(*Circulation*. 2013;127:1209-1218.)**

Key Words: atherosclerosis ■ cholesterol ■ plasminogen

Macrophage-derived foam cell formation, a hallmark of the progression of atherosclerosis, begins with recruitment of monocytes into the subendothelial space of affected blood vessels. In the cytokine-rich subendothelial microenvironment, monocytes differentiate into macrophages with concomitant expression of proteins that mediate the uptake of modified lipoproteins and retention of cholesterol in the cells.[1,2] Among the genes upregulated during foam cell formation are scavenger (CD36, MSRA, CD68) and phagocytic (phosphatidylserine receptor, Fcγ, SRB1, ATP-binding cassette transporter [ABCA1]) receptors that mediate uptake of oxidized low-density lipoprotein (OxLDL), nuclear receptors (peroxisome proliferator-activated receptor [PPAR] and CCAAT/enhancer binding protein [CEBP]) that regulate expression of the receptors involved in LDL uptake, and genes involved in eicasanoid (eg, hydroxyeicosatetraenoic acids, leukotrienes) biosynthesis that activate the aforementioned nuclear receptors.

Editorial see p 1173
Clinical Perspective on p 1218

Plasminogen (Plg) is synthesized primarily by the liver and circulates in the blood at 1 to 2 μmol/L.[3,4] Plg is converted to an active serine protease, plasmin, by Plg activators, a transition that is influenced by interaction of Plg with C-terminal lysines of extracellular matrix and cell-surface Plg receptors (Plg-Rs). Hence, blockade of Plg with lysine analogs such as tranexamic acid or antibodies directed at the C-terminal lysine region of Plg-Rs blocks the interaction of Plg with cells and dampens plasmin generation.[5]

Beyond the extracellular proteolytic functions of Plg,[6] its interaction with cells can trigger intracellular signaling.[7,8] Plasmin activates 5-lipoxygenase (5-LO),[7,9] a key enzyme in leukotriene biosynthesis that generates eicosanoids, including leukotriene B_4 (LTB_4), a biologically active lipid mediator associated with cardiovascular pathologies.[10] Indeed, the predominant source of blood leukotrienes is inflammatory cells such as activated monocytes and macrophages.[10] 5-LO and LTB_4 contribute to the formation of atherosclerotic lesions in both $ApoE^{-/-}$ and $Ldr^{-/-}$ mouse models by enhancing inflammation and foam cell formation.[11,12]

A number of studies in humans have established a direct association between Plg levels or plasmin activity and the incidence of coronary artery disease. As examples, 2 separate perspective cohort studies, FINRISK '92 Hemostasis Study[13] and the Atherosclerosis Risk in Communities Study (ARIC),[14] showed that Plg levels were an independent risk factor for coronary artery disease. A separate cohort study[15] reported that the level of plasmin-α2-antiplasmin, a marker of plasmin generation, was directly associated with abnormal ankle-arm index, a measure of atherosclerosis. Other studies also confirm a direct correlation between blood levels of plasmin–α2

Received October 4, 2012; accepted January 14, 2013.

From the Department of Molecular Cardiology, Cleveland Clinic, Cleveland, OH (R.D., S.G., C.D., M.F., E.F.P.); and Case Cardiovascular Research Institute, Case Western Reserve University, Cleveland, OH (G.H.M., M.K.J.).

*S. Ganapathy and Dr Mahabeleshwar contributed equally.

The online-only Data Supplement is available with this article at http://circ.ahajournals.org/lookup/suppl/doi:10.1161/CIRCULATIONAHA.112.001214/-/DC1.

Correspondence to Edward F. Plow, PhD, Department of Molecular Cardiology, 9500 Euclid Ave, NB-50, Cleveland, OH 44195. E-mail plowe@ccf.org

© 2013 American Heart Association, Inc.

Circulation **is available at http://circ.ahajournals.org** **DOI: 10.1161/CIRCULATIONAHA.112.001214**

Downloaded from http://circ.ahajournals.org/ at INSERM U460 UFR XAVIER BI on March 3, 2014

plasmin complex[16] or fibrin D-dimer[14,16,17] and coronary artery disease. The role of Plg in atherosclerosis has also been studied in Plg-deficient mice system.[18–20] In the most recently published study, Kremen et al[19] demonstrated that Plg knockout mice in an ApoE$^{-/-}$ background displayed a marked reduction in aortic lesion area. However, the mechanism by which Plg influenced lesion development remains unknown. Here, we present in vitro and in vivo studies that demonstrate that Plg is critical for transforming macrophages into lipid-laden foam cells. Surprisingly, this effect depends on alteration of expression of key genes associated with cholesterol accumulation into macrophages.

Methods

Animals

All animal experiments were performed under institutionally approved protocols. Tenth-generation male and female Plg$^{+/+}$ and Plg$^{-/-}$ mice[4] in C57BL/6J were used, beginning at 8 to 10 weeks of age. ApoE$^{-/-}$ mice in C57BL/6J background were from Jackson Laboratories (Bar Harbor, ME) and bred with Plg$^{+/-}$ mice to obtain ApoE$^{-/-}$Plg$^{+/+}$ and ApoE$^{-/-}$Plg$^{-/-}$ mice. Male mice with <20% variation in weight among ApoE$^{-/-}$ and ApoE$^{-/-}$Plg$^{-/-}$ genotypes were used. Four-week-old ApoE$^{-/-}$ and Plg$^{-/-}$ApoE$^{-/-}$ mice were fed either a normal chow diet (CD) or a high-cholesterol diet (HCD; containing 0.15% added cholesterol and 42% milk fat, TD88137, Harlan-Teklad) for 6 weeks. Plg mutant mice in which the active-site Ser was replaced by Ala[21] were kindly provided by Drs Ploplis and Castellino (University of Notre Dame). CD36$^{-/-}$ (10 times backcrossed to C57Bl/6) mice have previously been described.[22]

Ex Vivo and In Vivo Foam Cell Formation

Ex vivo foam cell formation was assessed with thioglycollate-elicited peritoneal macrophages and serum from Plg$^{+/+}$ or Plg$^{-/-}$ mice. In vivo foam cell formation was performed with ApoE$^{-/-}$ and ApoE$^{-/-}$Plg$^{-/-}$ mice. Specific protocols for both assays are expanded in the online-only Data Supplement. The isolation and use of human blood monocyte–derived macrophages, THP-1, and RAW264.7 cell lines are explained in the online-only Data Supplement.

OxLDL Binding and Internalization

These assays using OxLDL fluorescently labeled with 1,1′-dioctadecyl-1-3,3,3′,3′-tetramethylindocarbocyanine perchlorate (Dil, Biomedical Technologies, Inc) are described in the online-only Data Supplement.

In Vivo Transfer of Macrophages

This analysis is detailed in the online-only Data Supplement.

Real-Time Reverse Transcription–Polymerase Chain Reaction

Isolated RNA from variously treated cells was transcribed into cDNA. Quantitative polymerase chain reaction was performed on cDNA with specific oligonucleotides (Table I in the online-only Data Supplement).

Western Blots

Total cell lysates were analyzed by Western blotting (detailed in the online-only Data Supplement) using anti-CD36 antibody (R&D or Novus Biologicals).

Fluorescence-Activated Cell Sorter Analysis

Cell surface expression of CD36 was analyzed by flow cytometry (detailed in the online-only Data Supplement) using FITC-labeled rat anti-mouse CD36 (Cayman, Ann Arbor, MI).

Blood Cholesterol Quantification

Mice were fasted for 16 hours before blood collection from tail clips. Plasma from the mice was used to measure total LDL/very low density lipoprotein (VLDL) and high-density lipoprotein content with quantification kits from Biovision (Milpitas, CA).

Serum LTB_4 Measurement

Serum LTB_4 levels were quantified with a kit from Cayman Chemical.

Statistical Analysis

A 2-tailed *t* test was used in comparing 2 groups, and differences between multiple groups were evaluated with either a 1-way ANOVA or a 2-way ANOVA test followed by the Tukey multiple-comparison test (detailed in the online-only Data Supplement).

Results

Plg Regulates Macrophage Foam Cell Formation

Plg was shown to support lipid core growth in a murine diet-induced atherosclerosis model.[19,20] To dissect the mechanism for this proatherogenic activity, we assessed lipid uptake by thioglycollate-elicited peritoneal macrophages derived from Plg$^{+/+}$ or Plg$^{-/-}$ mice on exposure to OxLDL, culturing the cells in autologous serum. Lipid uptake, assessed by Oil Red O (ORO) staining, was dramatically impaired by macrophages derived from Plg$^{-/-}$ compared with Plg$^{+/+}$ mice (Figure 1A). Quantitatively, the reduction in total cholesterol in macrophages derived from Plg$^{-/-}$ mice was 62.5% (P<0.001) less than in wild-type (WT) macrophages (Figure 1B).

Mixing experiments were performed with macrophages derived from Plg$^{+/+}$ mice cultured in serum derived from Plg$^{+/+}$ and Plg$^{-/-}$ mice. OxLDL induced no lipid accumulation in the absence of serum (Figure 1C and 1D). Macrophages cultured in Plg$^{+/+}$ serum took up OxLDL and developed a rounded foam cell appearance (Figure 1C and 1D). In contrast, Plg$^{+/+}$ macrophages cultured in Plg$^{-/-}$ serum displayed reduced ORO staining and cholesterol content (48.4% reduction; P<0.001) compared with the same (WT) macrophages cultured in Plg$^{+/+}$ serum. The reduced ability of Plg$^{-/-}$ serum to support lipid uptake was restored when Glu-Plg was added at its physiological concentration (1 μmol/L[4]) to Plg$^{-/-}$ serum.

The influence of Plg on cholesterol accumulation also was observed with human monocyte–derived macrophages. In the presence of OxLDL, human monocyte–derived macrophages accumulated lipids when cultured in autologous serum as indicated by ORO staining (Figure 1E) and total cholesterol quantification (Figure 1F). Depletion of Plg from the serum on lysine-Sepharose lowered lipid accumulation by 49.1% (Figure 1F), and supplementing the depleted serum with Plg re-established cholesterol accumulation. A similar dependence of lipid uptake on Plg was observed with human monocytoid THP-1 cells (Figure IA in the online-only Data Supplement) and mouse macrophage RAW264.7 cells (Figure IB in the online-only Data Supplement). The RAW264.7 cells cultured in only 1% Nutridoma still showed an increased lipid accumulation in response to OxLDL on addition of Plg.

Functional Requirements for Plg-Mediated Foam Cell Formation

The requirement for proteolytic activity of plasmin in foam cell formation was evaluated by 2 approaches. First, aprotinin, a serine protease inhibitor, added to macrophages cultured in

Downloaded from http://circ.ahajournals.org/ at INSERM U460 UFR XAVIER BI on March 3, 2014

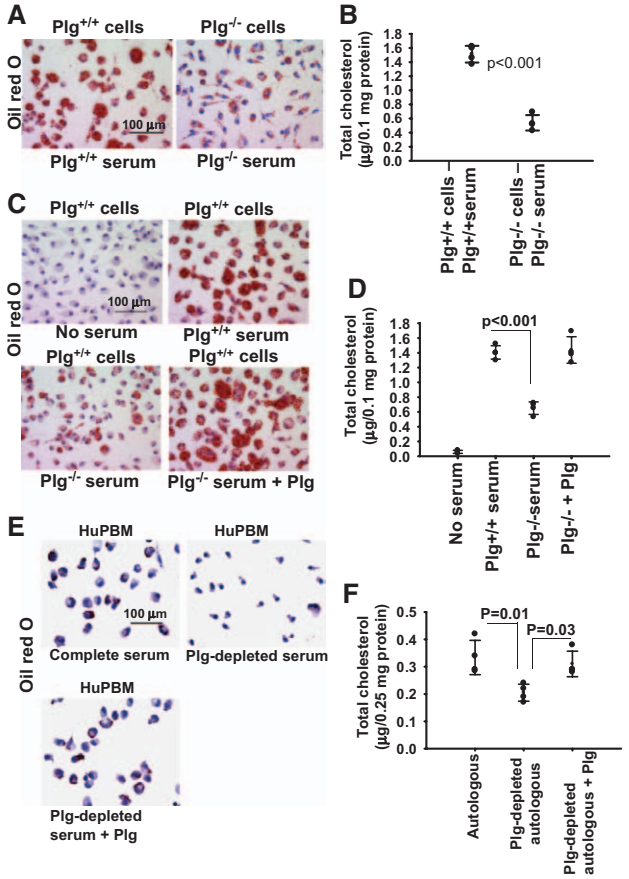

Figure 1. Plasminogen (Plg) regulates lipid uptake by macrophages and foam cell formation. **A** through **D**, Thioglycollate-elicited peritoneal macrophages from $Plg^{+/+}$ or $Plg^{-/-}$ mice were induced to form foam cell with oxidized low-density lipoprotein (OxLDL) in the absence of serum or in the presence of serum derived from either $Plg^{+/+}$ or $Plg^{-/-}$ mice. **E** and **F**, Human monocyte–derived macrophages (HuPBMs) were induced to form foam cells by the addition of OxLDL and cultured in autologous serum or autologous serum depleted of Plg. In some murine or human cultures, Plg-deficient serum was supplemented with 1 μmol/L Glu-Plg. **A**, **C**, and **E**, Oil Red O staining of foam cells at original magnification ×40. Images are representative of 2 independent experiments. **B**, **D**, and **F**, Total cholesterol was measured in foam cells. Dots represent individual data points; the number of replicates is 4. Error bars are ±SD of the mean.

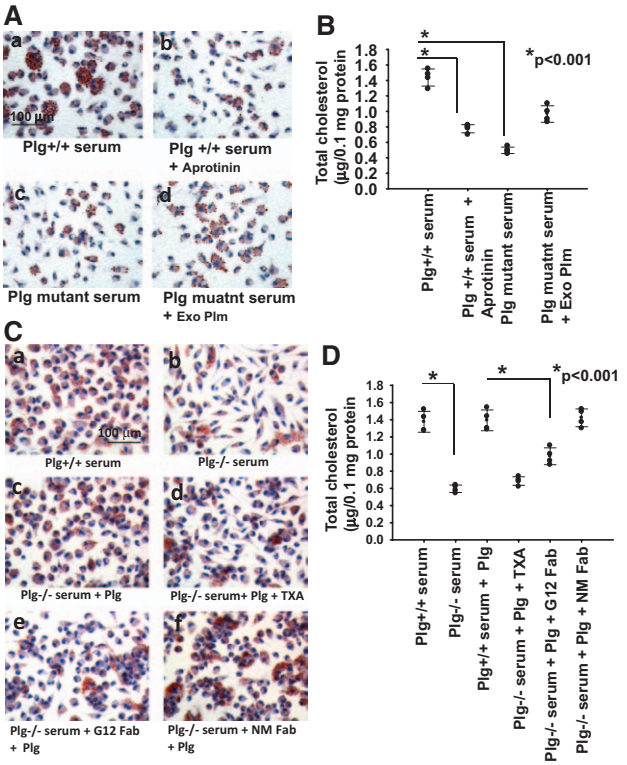

Figure 2. Plasminogen (Plg) receptors and plasmin activity are required for Plg-mediated foam cell formation. **A** and **B**, Thioglycollate-elicited macrophages from $Plg^{+/+}$ mice were untreated or treated with aprotinin (100 KIU/mL). The cells were then allowed to form foam cells by adding oxidized low-density lipoprotein (OxLDL) in the presence of serum derived from $Plg^{+/+}$ mice or Plg mutant mice (expressing active-site mutant of Plg). **C** and **D**, Tranexamic acid (TXA; 200 μmol/L), Fab fragments of anti-H2B monoclonal antibody (G12; 8 μmol/L), nonimmune mouse IgG Fab (NM; 8 μmol/L), or buffer was added to thioglycollate-elicited macrophages, and foam cell formation was induced with OxLDL. **A** and **C**, Oil Red O staining of foam cells at original ×40 magnification. Images are representative of 2 independent experiments. **B** and **D**, Total cholesterol was measured in the cultured macrophages. Each dot is 1 of 4 replicates; error bars are ±SD of the mean. Exo Plm indicates exogenous plasmin.

$Plg^{+/+}$ serum (Figure 2A and 2B) inhibited cholesterol accumulation by 48.4% ($P<0.001$). Second, cholesterol accumulation by macrophages cultured in serum from mice expressing an active-site mutant of Plg,[21] which is cleavable by Plg activators but does not form an active enzyme (Figure 2Ac and 2B), was suppressed by 67.7% compared with WT serum ($P<0.001$). Addition of exogenous Plg to the serum from Plg mutant mice enhanced ORO staining and cholesterol uptake (33% recovery; Figure 2Ad and 2B), but not as effectively as the addition of the same amount of Plg to $Plg^{-/-}$ serum (Figure 1C and 1D). This partial restoration of lipid uptake may reflect competition of mutant Plg with added WT Plg.

Many cellular functions of Plg depend on its interaction with Plg-Rs via its kringle-associated lysine binding sites, and tranexamic acid, a lysine analog, blocks Plg binding to most Plg-Rs on macrophages. The recovery of foam cell formation on the addition of Plg to macrophages cultured in $Plg^{-/-}$ serum (Figure 2Cc and 2D) was inhibited by >90% ($P<0.001$) by tranexamic acid (Figure 2Cd and 2D). Multiple Plg-Rs have been implicated in the binding of Plg to macrophages, and among these, histone H2B plays a particularly prominent in Plg binding.[23] Fab fragments of the monoclonal antibody G12 raised to the C-terminal peptide of H2B (Figure 2C and 2D) inhibited the ability of Plg to enhance cholesterol accumulation by macrophages by 53% ($P<0.001$) compared with nonimmune Fab (Figure 2Cf and 2D). Hence, the ability of Plg to enhance foam cell formation is dependent on its interaction with the Plg-Rs. H2B does contribute and other Plg-Rs may contribute to this response.

Plg Supports Binding and Internalization of OxLDL

To assess the effects of Plg on lipoprotein binding and/or internalization, thioglycollate-inflamed peritoneal macrophages were incubated with various concentrations of fluorescently tagged OxLDL (Dil-OxLDL) for 30 minutes at 4°C for binding and 2 hours at 37°C for internalization. By flow

Downloaded from http://circ.ahajournals.org/ at INSERM U460 UFR XAVIER BI on March 3, 2014

cytometry, macrophages from Plg$^{-/-}$ mice showed reduced binding (Figure 3A) and internalization (Figure 3B) compared with Plg$^{+/+}$ macrophages. At 10 μg/mL, Plg$^{-/-}$-derived macrophages bound 2.5-fold (P≤0.04) less and took up 1.7-fold (P≤0.001) less Dil-OxLDL than Plg$^{-/-}$ mice. Binding and uptake results were confirmed on WT macrophages cultured in serum derived from either Plg$^{+/+}$ or Plg$^{-/-}$ mice for 2 days. Both parameters were lowered (at 10 μg/mL Dil-OxLDL, 2-fold, P<0.001 for binding, and 2.2-fold, P≤0.003 for internalization) in macrophages cultured in Plg$^{-/-}$ compared with Plg$^{+/+}$ serum (Figure 3C and 3D).

To consider whether plasmin might modify OxLDL and aid in cholesterol accumulation, we cultured the macrophages in Plg$^{+/+}$ or Plg$^{-/-}$ serum and then washed the cells thoroughly and measured Dil-OxLDL binding in the absence of Plg. Binding to cells cultured in the Plg$^{-/-}$ serum was still 50% less (P<0.001) than macrophages cultured in Plg$^{+/+}$ serum (Figure 3E). Macrophages cultured in Plg$^{-/-}$ serum supplemented with exogenous Plg recovered their capacity to bind Dil-OxLDL, and inclusion of aprotinin with the exogenous Plg during culture inhibited this recovery. Additionally, macrophages cultured in serum from Plg mutant mice bound 62% less Dil-OxLDL (P<0.001) compared with macrophages cultured in Plg$^{+/+}$ serum. These differences correlated well with cholesterol accumulation and foam cell formation (Figures 1 and 2).

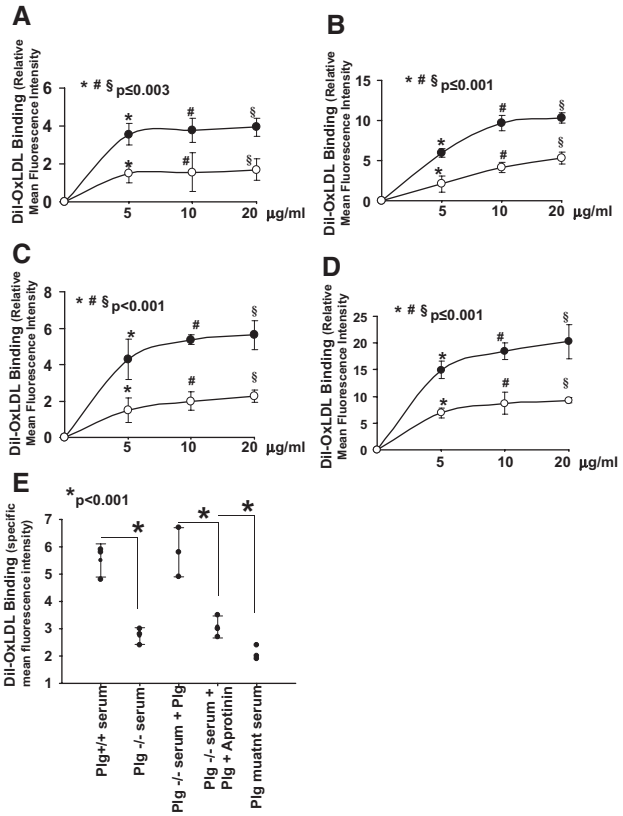

Figure 3. Role of plasminogen (Plg) in oxidized low-density lipoprotein (OxLDL) binding and internalization. **A** and **B**, Thioglycollate-elicited peritoneal macrophages derived from Plg$^{+/+}$ (•) or Plg$^{-/-}$ (○)mice were allowed to bind (**A**; 30 minutes at 4°C) or to internalize (**B**; 2 hours at 37°C) Dil-OxLDL. **C** and **D**, Peritoneal macrophages from Plg$^{+/+}$ mice were cultured in the presence of serum derived from Plg$^{+/+}$ (•) or Plg$^{-/-}$ mice (○) and then allowed to bind (**C**) or to internalize (**D**) varying concentrations of Dil-OxLDL. Points are ±SD of means from triplicate samples. **E**, Macrophages derived from Plg$^{+/+}$ mice were cultured in Plg$^{+/+}$, Plg$^{-/-}$ serum, or serum from Plg active-site mutant mice. In some panels, Plg (1 μmol/L) or aprotinin (blocks plasmin activity) was added. Cells were washed and allowed to bind Dil-OxLDL in the presence or absence of excess unlabeled OxLDL. Bound or internalized Dil-OxLDL was measured by flow cytometry. Specific binding values are displayed and were obtained by subtracting residual nonspecific binding in the presence of excess OxLDL. Each dot is an average of triplicates.

Foam Cell Formation In Vivo Is Impaired by the Absence of Plg

To translate our observations into an in vivo setting, we crossed the Plg$^{-/-}$ and ApoE$^{-/-}$ mice and maintained the resulting ApoE$^{-/-}$Plg$^{-/-}$ and ApoE$^{-/-}$ mice on the CD or HCD. After 6 weeks, plasma LDL/VLDL was elevated in mice of both backgrounds fed the HCD compared with those fed the CD, and high-density lipoprotein was lower in ApoE$^{-/-}$ mice fed the HCD compared with those fed the CD (Table II in the online-only Data Supplement). Plasma LDL/VLDL levels were similar in the Plg-deficient and Plg-replete ApoE$^{-/-}$ backgrounds, but the high-density lipoprotein level was lower (P≤0.01) in Plg $^{-/-}$ApoE$^{-/-}$ mice compared with ApoE$^{-/-}$ on both the CD and HCD (Table II in the online-only Data Supplement). Thioglycollate was used to recruit peritoneal macrophages in these mice, and equal numbers of cells were evaluated for lipid and total cholesterol content. Regardless of genotype, macrophages derived from mice fed the HCD showed increased lipid staining and a higher intracellular cholesterol than those fed the CD (Figure 4A and 4B). However, internal lipid staining and total cholesterol content were dramatically reduced in macrophages derived from ApoE$^{-/-}$Plg$^{-/-}$ mice compared with ApoE$^{-/-}$ mice (Figure

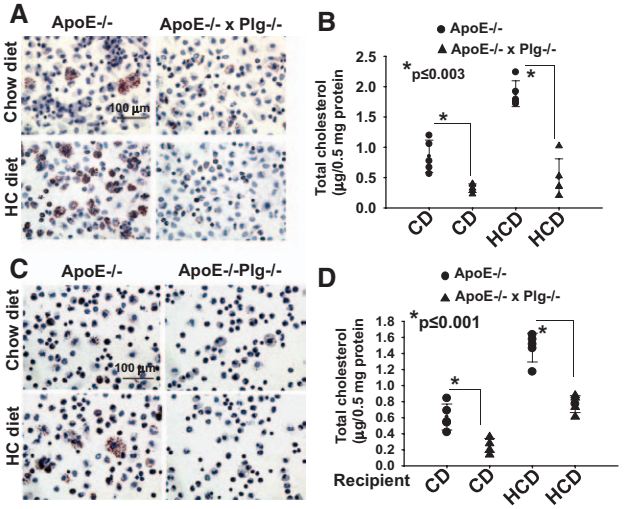

Figure 4. Effect of plasminogen (Plg) deficiency on foam cell formation in vivo. **A** and **B**, Foam cells were measured in thioglycollate-elicited peritoneal macrophages derived from ApoE$^{-/-}$ or ApoE$^{-/-}$Plg$^{-/-}$ mice fed either a chow diet (CD) or a high-cholesterol diet (HCD). **C** and **D**, Foam cell formation was assessed by macrophages transferred to ApoE$^{-/-}$ and ApoE$^{-/-}$/Plg$^{-/-}$ recipient mice that had been fed a CD or an HCD. **A** and **C**, Oil Red O staining at an original ×40 magnification. Images are representative of cells from 5 mice. **B** and **D**, Quantification of total cholesterol. Each dot represents a data point from 1 of 5 mice. Error bars are the SD of the means.

Downloaded from http://circ.ahajournals.org/ at INSERM U460 UFR XAVIER BI on March 3, 2014

4A and 4B). These differences in lipid accumulation in the Plg$^{-/-}$ background were observed in mice fed either the CD (60%; $P \leq 0.003$) or the HCD (68.3%; $P \leq 0.003$). Thus, cholesterol accumulation in macrophages in vivo is strongly influenced by Plg.

We considered whether the observed in vivo differences in lipid accumulation might reflect differences in the macrophage populations recruited into the peritoneal cavity of ApoE$^{-/-}$ and Plg$^{-/-}$ApoE$^{-/-}$ mice and performed macrophage transfer experiments.[24] Thioglycollate-elicited macrophages derived from Plg$^{+/+}$ mice were injected into the peritoneal cavity of recipient ApoE$^{-/-}$ and ApoE$^{-/-}$Plg$^{-/-}$ mice that had been maintained on the CD or HCD for 6 weeks. Cells were recovered 3 days after thioglycollate stimulation and analyzed for lipid accumulation. Reduction of ORO staining (Figure 4C) and cholesterol content (42.1%, $P \leq 0.001$ on CD, and 48%, $P \leq 0.001$ on HCD; Figure 4D) were observed in transferred macrophages obtained from ApoE$^{-/-}$Plg$^{-/-}$ recipient mice compared with ApoE$^{-/-}$ recipient mice. Additionally, levels of Plg in the peritoneal fluid were found to be the same in ApoE$^{-/-}$ mice on CD and mice on a high-fat diet (607.1 versus 586.5 ng/mL lavage; $P > 0.7$). Plg was not detected in the lavage from ApoE$^{-/-}$Plg$^{-/-}$ mice in either diet. Thus, the differences in cholesterol content of macrophages were consequences of both diet and Plg deficiency and were not due to differences in the population of recruited macrophages or to diet-associated differences in the peritoneal content of Plg. We also measured the levels of LDL/VLDL in the peritoneal lavage from these mice. In CD-fed mice, VLDL and LDL in the lavage were the same in ApoE$^{-/-}$ and ApoE$^{-/-}$Plg$^{-/-}$ mice (38.2 versus 41.2 mg/mL in 1.5 mL peritoneal wash), yet these mice still showed a difference in foam cell formation (Figure 4C and 4D), supporting the direct role of Plg in lipid uptake. In the HCD-fed mice, a 2-fold difference in VLDL/LDL levels in the ApoE$^{-/-}$Plg$^{-/-}$ compared with ApoE$^{-/-}$ mice (81 versus 38.1 mg/mL) was noted. Despite this difference in VLDL/LDL levels, the differences in cholesterol content were similar (42.1% and 48% reduction) in Plg$^{-/-}$ and Plg$^{+/+}$ mice regardless of diet.

Plg Regulates the Expression of Genes Involved in Foam Cell Formation

We next examined how Plg influences the expression of selected genes implicated in lipid metabolism. These included receptors involved in OxLDL uptake, CD36, MSRA and CD68; receptors involved in phagocytosis of OxLDL, immune complexes, and apoptotic bodies, represented by phosphatidylserine receptor, Fcγ receptor type 1, Fcγ receptor type II, SRB1, and ABCA1; and nuclear receptors known to regulate these receptors, including PPARγ, CEBPα, CEBPβ, and TR4.[1,2,25,26] In the absence of OxLDL, no differences were observed in the expression levels of genes tested between cells cultured in Plg$^{+/+}$ and Plg$^{-/-}$ conditions except CD36 (Figure 5A); CD36 expression was inhibited by 30% (P=0.04) in Plg$^{-/-}$ serum compared with Plg$^{+/+}$ serum. Expression levels of tested genes were consistently higher on stimulation with OxLDL in macrophages cultured in Plg$^{+/+}$ serum compared with unstimulated cells ($P \leq 0.01$). The exceptions were phosphatidylserine receptor and CEBPα (Figure 5B and 5C), which did not change on OxLDL stimulation. In the absence

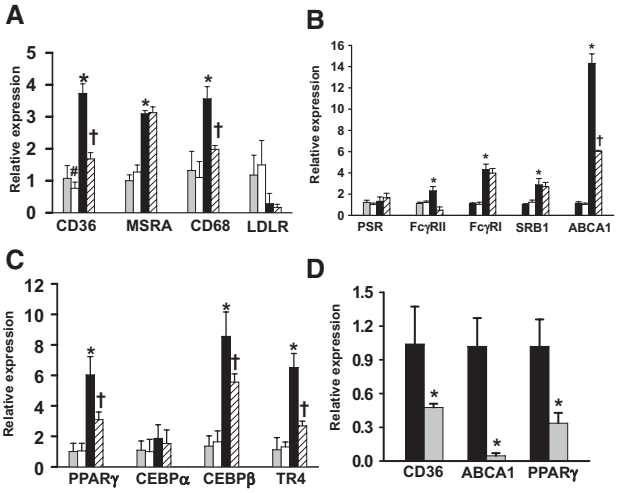

Figure 5. Plasminogen (Plg) deficiency causes reduced expression of genes involved in lipid uptake. **A** through **C**, Real-time polymerase chain reaction quantification of transcripts of genes related to lipid uptake (**A**), phagocytosis (**B**), or nuclear receptors (**C**) on foam cells treated with either Plg$^{+/+}$ or Plg$^{-/-}$ mouse–derived serum. Gray bars indicate Plg$^{+/+}$ serum, oxidized low-density lipoprotein (OxLDL) untreated; white bars, Plg$^{-/-}$ serum, OxLDL untreated; black bars, Plg$^{+/+}$ serum, OxLDL treated; and striated bars, Plg$^{-/-}$ serum, OxLDL treated. Bars are mean±SD of triplicates. Data are representative of 2 independent experiments. *$P \leq 0.01$ vs Plg$^{+/+}$ serum; #P=0.04 vs Plg$^{+/+}$ serum; †$P < 0.002$ vs Plg$^{+/+}$ serum treated with OxLDL. **D**, Real-time polymerase chain reaction quantification on mRNA of transferred macrophages derived from hyperlipidemic ApoE$^{-/-}$ (black bars) and ApoE$^{-/-}$Plg$^{-/-}$ (gray bars) recipient mice. Bars are mean±SD of triplicates. mRNAs are pooled from macrophages derived from 5 mice. ABCA1 indicates ATP-binding cassette transporter; CEBP, CCAAT/enhancer binding protein; FcγRI, Fcγ receptor type 1; FcγRII, Fcγ receptor type II; and PPAR, peroxisome proliferator-activated receptor. *P<0.001 vs Plg$^{+/+}$ serum treated with OxLDL.

of Plg, OxLDL-mediated CD36 expression decreased by 57% (P=0.005) compared with Plg$^{+/+}$ serum (Figure 5A). Among other genes, OxLDL-mediated CD68 (Figure 5A), Fcγ receptor type II, and ABCA1 expression levels were significantly lower in the absence of Plg (Figure 5B). Among the nuclear receptors, OxLDL induced upregulation of transcripts for PPARγ, CEBPβ, and TR4 in macrophages, and all were suppressed in the Plg$^{-/-}$ environment (Figure 5C).

The expression levels of the most effected genes were further evaluated in macrophages derived from in vivo transfer experiments. Transcript levels of CD36, ABCA1, and PPARγ were significantly suppressed ($P \leq 0.01$) in ApoE$^{-/-}$Plg$^{-/-}$ recipient–derived macrophages compared with ApoE$^{-/-}$ recipient–derived macrophages (Figure 5D). Collectively, these results suggest that Plg might enhance macrophage accumulation of cholesterol by affecting the expression of various receptors involved in OxLDL uptake.

Role of CD36 in Plg-Mediated Cholesterol Accumulation

Among the scavenger receptors tested, CD36 expression was altered by the absence of Plg regardless of whether OxLDL was present (Figure 5A). At the protein level, Western blots of whole-cell lysates showed lower CD36 in macrophages from Plg$^{-/-}$ mice compared with Plg$^{+/+}$ mice (Figure 6A). By flow cytometry, CD36 cell-surface levels were 2.2-fold (P<0.001)

Downloaded from http://circ.ahajournals.org/ at INSERM U460 UFR XAVIER BI on March 3, 2014

lower in macrophages from Plg$^{-/-}$ compared with Plg$^{+/+}$ mice (Figure 6B). The expression of CD36 depends on the differentiation status of macrophages.[27] Plg$^{+/+}$ mouse–derived macrophages cultured for 2 days in Plg$^{+/+}$ serum showed a 2-fold higher CD36 protein expression than freshly isolated macrophages from Plg$^{+/+}$ mice at both the whole-cell (Figure 6C) and cell-surface levels (Figure 6D). However, CD36 expression did not increase from basal levels when these cells were cultured for 2 days in Plg$^{-/-}$ serum. On OxLDL treatment, CD36 expression was enhanced 2-fold in Plg$^{+/+}$ serum compared with untreated cells but inhibited by 45% when OxLDL-treated macrophages were cultured in Plg$^{-/-}$ serum (Figure 6C and 6D). These data suggest that CD36 gene and protein expression is regulated by Plg. Regulation of CD36 expression by Plg was confirmed with RAW264.7 cells grown in the absence of serum. When these cells were treated with 1 μmol/L Plg, their CD36 protein expression increased (Figure IIA in the online-only Data Supplement).

CD36 was further implicated in Plg-mediated OxLDL uptake and cholesterol accumulation. When macrophages derived from CD36$^{-/-}$ mice were cultured in Plg$^{-/-}$ serum, they showed little accumulation of lipid in response to OxLDL (Figure 6E), and the addition of Plg did not rescue cholesterol accumulation in CD36$^{-/-}$ macrophages as it did with CD36$^{+/+}$ cells (Figure 6E). Together, these data indicate that a major component of Plg-mediated foam cell formation is dependent on its regulation of CD36 expression.

Effect of Plg on LTB_4 Biosynthesis

LTB_4 influences many crucial steps in early development of atherosclerosis,[10-12] and Plg/plasmin induces monocyte production of several leukotrienes, including LTB_4.[9] We hypothesized that reduced LTB_4 production could be a mechanism underlying Plg-dependent foam cell formation. We first quantified LTB_4 levels in serum from Plg$^{-/-}$ and Plg$^{+/+}$ mice (Figure 7A). Serum from Plg$^{-/-}$ mice contained 2-fold less LTB_4 than serum from Plg$^{+/+}$ mice (1.8±0.2 versus 3.3±0.4 nmol/L; n=5; P<0.001). LTB_4 levels were also measured in ApoE$^{-/-}$ mice. LTB_4 levels were 2.3-fold higher (P <0.001) in ApoE$^{-/-}$ mice fed the HCD compared with animals fed the CD for 6 weeks (Figure 7B), consistent with previous reports.[28] Most notably, in ApoE$^{-/-}$Plg$^{-/-}$ mice, LTB_4 levels in serum were ≈40% lower in both CD-fed mice (1.7±0.4 nmol/L in ApoE$^{-/-}$Plg$^{-/-}$ mice versus 3.8±0.4 nmol/L in ApoE$^{-/-}$Plg$^{+/+}$ mice; n=5; P=0.03) and HCD-fed mice (4.4±1.2 nmol/L in ApoE$^{-/-}$Plg$^{-/-}$ mice versus 10.2±1.6 nmol/L in ApoE$^{-/-}$Plg$^{+/+}$ mice; n=5; P<0.001; Figure 7B). Additionally, in ApoE$^{-/-}$Plg$^{-/-}$ mice, LTB_4 levels in peritoneal fluid were 46% lower (0.06 versus 0.1 nmol/L in CD-fed mice and 0.2 nmol/L versus 0.4 nmol/L in HCD-fed mice) compared with ApoE$^{-/-}$ mice. Thus, Plg influences LTB_4 production in vivo.

LTB_4 Bypasses the Effects of Plg Deficiency on Foam Cell Formation and Gene Expression

Thioglycollate-elicited peritoneal macrophages were presented with OxLDL in Plg$^{+/+}$ or Plg$^{-/-}$ serum (Figure 7C and 7D) with or without supplemental Plg or LTB_4. The addition of Plg or LTB_4 overcame the suppressive effects of Plg deficiency (Figure 7C and 7D). As noted, macrophages grown in Plg$^{-/-}$ serum have less CD36 on their surface than macrophages in Plg$^{+/+}$ serum. The addition of either Plg or LTB_4 (500 nmol/L)[29] to the Plg$^{-/-}$ serum enhanced cell-surface expression of CD36 (Figure 7E and Figure IIB in the online-only Data Supplement). Adding Plg and LTB_4 together to Plg$^{-/-}$ serum did not have an additional effect on ORO staining (Figure 7C), cholesterol accumulation (Figure

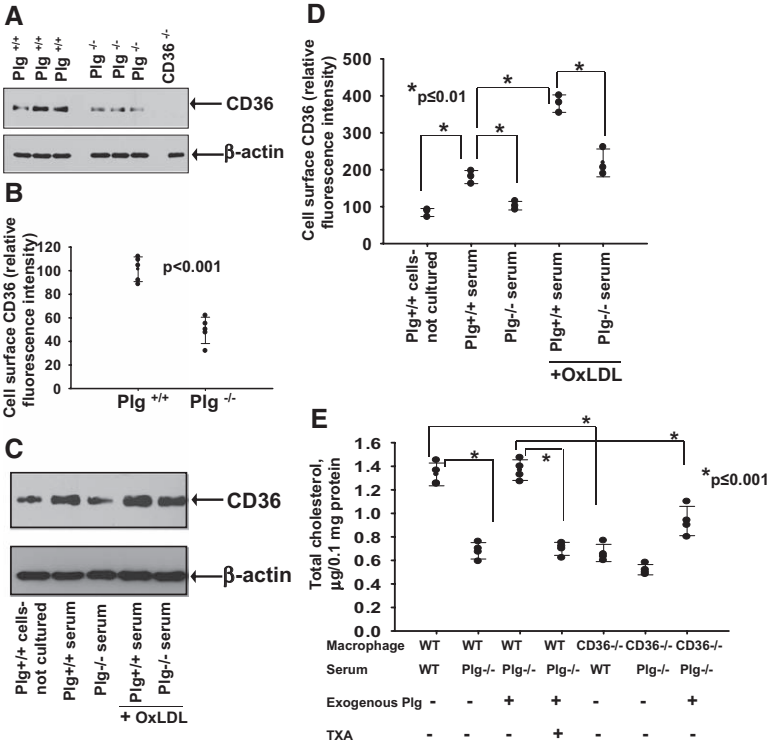

Figure 6. Role of CD36 in plasminogen (Plg)-mediated foam cell formation. **A**, Western blot for CD36 (**top**) of macrophages derived from either Plg$^{+/+}$ mice or Plg$^{-/-}$ mice. CD36$^{-/-}$ macrophages were analyzed as a negative control. **B**, Flow cytometry for cell surface CD36 of macrophages derived from either Plg$^{+/+}$ mice (n=5) or Plg$^{-/-}$ mice (n=5). Each dot is a data point from 1 of 5 mice. Error bars are mean±SD. **C** and **D**, Western blot (**C**, **top**) and flow cytometry (**D**) for CD36 on either freshly isolated macrophages derived from Plg$^{+/+}$ mice or macrophages cultured in Plg$^{+/+}$ mouse–derived serum in either the absence or presence of oxidized low-density lipoprotein (OxLDL). Dots are averages of triplicate values. Actin levels serve as loading controls (**A** and **C**, **bottom**). **E**, Total cholesterol quantification on OxLDL-treated macrophages from Plg$^{+/+}$ mice or CD36$^{-/-}$ mice cultured in either Plg$^{+/+}$ or Plg$^{-/-}$ serum in the absence or presence of Plg. Each dot is 1 of 4 replicates; error bars are the SD of the means. TXA indicates tranexamic acid.

Downloaded from http://circ.ahajournals.org/ at INSERM U460 UFR XAVIER BI on March 3, 2014

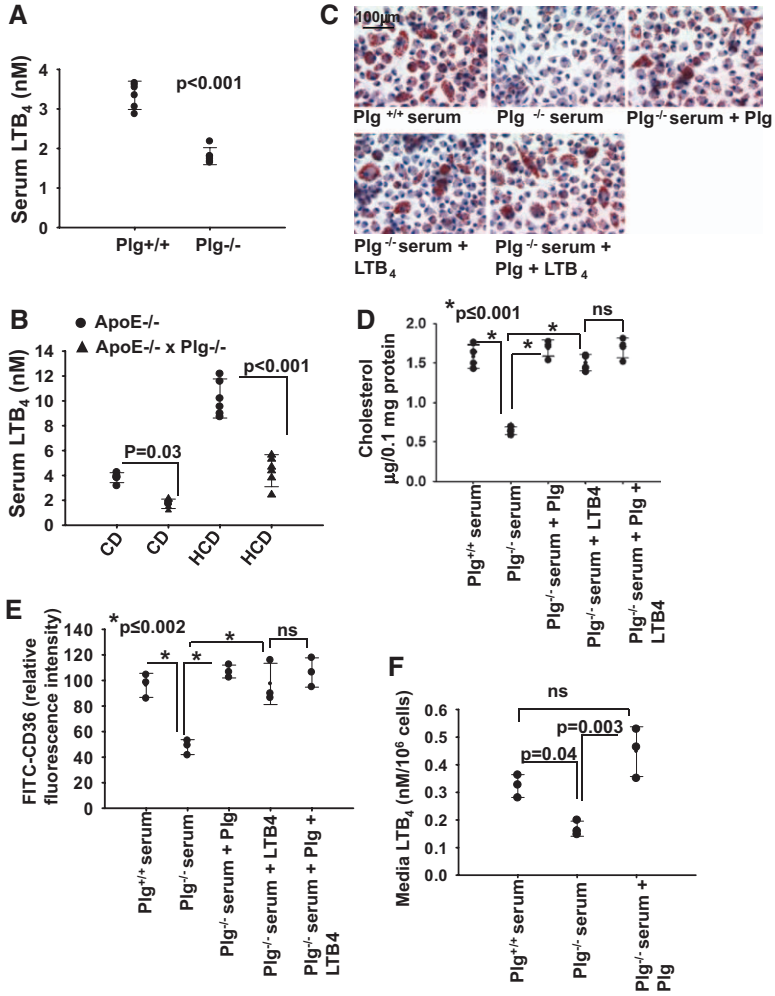

Figure 7. Relationship between plasminogen (Plg), leukotriene B_4 (LTB_4), and foam cell formation. **A**, Serum LTB_4 levels in thioglycollate-treated $Plg^{+/+}$ and $Plg^{-/-}$ mice. **B**, Serum LTB_4 levels in $ApoE^{-/-}$ mice or $Plg^{-/-}ApoE^{-/-}$ mice maintained on a high-cholesterol diet (HCD) or a chow diet (CD). Error bars are mean±SD from 5 mice. **C** through **E**, Oxidized low-density lipoprotein (OxLDL) induced foam cell formation by thioglycollate-elicited macrophages in $Plg^{+/+}$ serum or $Plg^{-/-}$ serum with or without added Plg (1 μmol/L) and LTB_4 (500 nmol/L). **C**, Oil Red O staining (original magnification ×40). Images are representative of 2 independent experiments. **D**, Total cholesterol quantification. Each dot is the data point from 1 of 4 individual wells. Error bars are the SD of means. **E**, Flow cytometry for surface CD36 expression. Bars are mean fluorescence intensities ±SD of triplicates. **F**, $Plg^{+/+}$ mouse–derived macrophages were cultured in serum derived from $Plg^{+/+}$ or $Plg^{-/-}$ mice in the absence or presence of Plg. Culture media were collected and LTB_4 levels measured. Each dot is the value for 3 independent experiments. Error bars are ±SD of means.

7D), or CD36 expression (Figure 7E and Figure IIB in the online-only Data) compared with LTB_4 alone, suggesting that LTB_4 is a downstream effector of Plg. When Plg was added to $Plg^{-/-}$ culture media, LTB_4 levels were fully recovered (Figure 7F).

5-LO–catalyzed LTB_4 synthesis requires an integral membrane protein, 5-LO activating protein. MK886 blocks LTB_4 secretion by inhibiting 5-LO activating protein activity.[30] When RAW264.7 cells were pretreated with MK886 and then with Plg, Plg-mediated upregulation of CD36 protein expression was completely suppressed at 500 nmol/L MK886 (Figure IIB in the online-only Data Supplement). LTB_4 can signal intracellularly or by binding to the G-protein–coupled receptors BLT_1 and BLT_2. Blocking BLT_1 (the higher-affinity LTB_4 receptor) with 2 unrelated inhibitors, LY293111 and U-75302, reduced Plg-mediated CD36 expression (75% with LY293111 and >90% with U-75302; Figure III in the online-only Data Supplement), suggesting that Plg-induced LTB_4 acts primarily via its extracellular release and interaction with BLT_1. In addition to LTB_4, Plg induces biosynthesis of cysteinyl-LTs [9]. Adding LTE_4, the most stable of the cysteinyl-LTs, did not enhance CD36 expression in RAW264.7 cells (Figure IV in the online-only Data Supplement), suggesting that between these 2 leukotrienes, the effect of Plg on CD36 expression depends on LTB_4.

Discussion

It is now clear that the role of Plg in vivo extends well beyond its function in fibrinolysis. By virtue of its capacity to degrade various extracellular matrix proteins, to activate certain MMPs, and to cleave secreted growth factors, Plg facilitates tissue reorganization and enhances cell migration.[3,5,6] In the present study, we report an unexpected effect of Plg on the capacity of macrophages to take up lipids and become foam cells. Surprisingly, Plg exerts these effects by controlling the expression of genes involved in OxLDL uptake by macrophages, most notably CD36, and this regulation is dependent on Plg-dependent activation of the 5-LO biosynthetic pathway. Thus, we have assigned a novel function to Plg in macrophage biology and have begun to define the molecular pathway underlying this function.

The importance of Plg in cholesterol accumulation was demonstrated with primary cells and cell lines of murine (peritoneal macrophages and RAW264.7 cells) and human (human monocyte–derived macrophages and THP-1) origin. With all these cells, culture in absence of Plg reduced ORO staining and cholesterol content in response to OxLDL compared with presence of Plg, and supplementing the Plg-deficient media with exogenous Plg overcame this suppression. Decreased cholesterol accumulation by macrophages under Plg-deficient conditions was very extensive (eg, cholesterol

Downloaded from http://circ.ahajournals.org/ at INSERM U460 UFR XAVIER BI on March 3, 2014

accumulation was reduced by 60% in macrophages from $Plg^{-/-}ApoE^{-/-}$ mice compared with those derived from $Plg^{+/+}ApoE^{-/-}$ mice). The pathway giving rise to residual cholesterol uptake in the absence of Plg is unknown. SRA1 expression was unaffected by the absence of Plg but was induced by OxLDL, and it is a candidate for mediating Plg-independent cholesterol accumulation. Growth factors such as insulin[31] and many cytokines like interleukin-10[32] also support foam cell formation and could contribute to Plg-independent lipid uptake. The molecular and cellular requirements for fat cell formation during adipogenesis often parallel those for macrophage transformation into foam cells. Hints about a possible role for Plg in lipid uptake can be derived from 2 prior studies of adipogenesis. Selvarajan et al[33] described a role for Plg in lipid absorption during preadipocyte differentiation to adipocytes, and Hoover-Plow et al[34] demonstrated reduced body weight and less accumulation of fat in $Plg^{-/-}$ compared with $Plg^{+/+}$ mice. Thus, the influence of Plg on lipid uptake may not be restricted to macrophages.

Correlating with Plg-dependent changes in cholesterol accumulation, binding and internalization of OxLDL were also impaired in the absence of Plg. In 1 arm of these studies, the Dil-OxLDL tracer was not directly exposed to Plg, yet macrophages cultured in Plg-deficient culture conditions showed reduced binding. These data suggest that the primary role of Plg is to affect the capacity of the macrophages to take up OxLDL rather than to modify the OxLDL ligand. Nevertheless, we do not exclude the possibility that plasmin may modify OxLDL over the 24 to 48 hours of the foam cell formation assays. Consistent with binding data among the tested scavenger receptors, mRNA and protein levels of the CD36 molecule were significantly suppressed in macrophages derived from $Plg^{-/-}$ mice compared with $Plg^{+/+}$ mice or in WT macrophages cultured in $Plg^{-/-}$ serum. CD36 accounts for almost 80% of foam cell formation by OxLDL generated by a myeloperoxidase-hydrogen peroxide-nitrite pathway[35] and 60% of OxLDL generated by copper oxidation.[22] Furthermore, studies of hypercholesterolemic $CD36^{-/-}$ mice have shown the importance of this receptor in uptake of OxLDL and foam cell formation.[22] We verified the role of CD36 in Plg-dependent foam cell formation using macrophages from CD36 knockout mice. The addition of exogenous Plg to Plg-deficient medium, which fully rescued cholesterol accumulation in WT macrophages, had little effect on CD36 knockout macrophages.

5-LO and its product, LTB_4, have been implicated in CD36 expression.[12] We found a reduced level of LTB_4 in serum from thioglycollate-treated $Plg^{-/-}$ compared with $Plg^{+/+}$ mice. This influence of Plg in LTB_4 biosynthesis was also substantiated in proatherogenic $ApoE^{-/-}$ mice, in which reduced LTB_4 levels were observed in serum of $ApoE^{-/-}Plg^{-/-}$ mice compared with $ApoE^{-/-}$ mice. Of particular note, we found that the addition of LTB_4 to Plg-deficient cultures overcame the reduction in cholesterol accumulation by macrophages. The effects of Plg and LTB_4 on cholesterol accumulation and CD36 expression suggest that these molecules function in the same pathway because LTB_4+Plg did not have an additive effect. Additionally, Plg-mediated CD36 expression required BLT_1, a high-affinity LTB_4 receptor. These data support the model depicted in Figure 8.

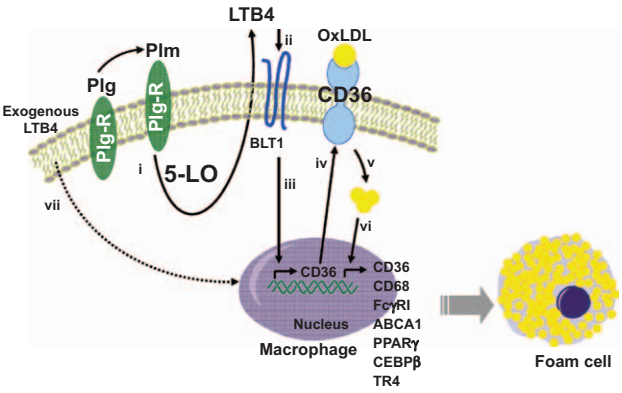

Figure 8. The plasminogen (Plg)-dependent pathway of foam cell formation. Plg binding to Plg receptors (Plg-Rs) activates 5-lipoxygenase (5-LO) in a plasmin (Plm)-dependent manner and leads to leukotriene B_4 (LTB_4) production and secretion by the macrophage (i). Secreted LTB_4 binds to BLT_1 (ii) and activates transcription of the CD36 gene (iii), CD36 protein synthesis, and translocation to the cell membrane (iv). The increased expression of CD36 facilitates uptake of oxidized low-density lipoprotein (OxLDL) and accumulation of cholesterol within the cells (v). The accumulated sterols induce a positive feedback loop for further cholesterol accumulation by enhancing the expression many relevant genes, including those for scavenger and phagocytic receptors and for the transcription factors that regulate these genes (vi). The Plg dependence of this pathway for CD36 expression and foam cell formation can be bypassed by exogenous LTB_4 (vii). This pathway shows the actions of Plg on a single cell, but released LTB_4 may affect adjacent cells. ABCA1 indicates ATP-binding cassette transporter; CEBP, CCAAT/enhancer binding protein; FcγRI, Fcγ receptor type 1; FcγRII, Fcγ receptor type II; and PPAR, peroxisome proliferator-activated receptor.

Accordingly, Plg and plasmin bind to receptors, including but not limited to H2B. Plasmin stimulates 5-LO activity, which in turn generates LTB_4. LTB_4, in part by releasing from the cell and engaging its high-affinity receptor, BLT_1, generates nuclear signals that enhance CD36 mRNA levels, protein, and cell-surface expression. The present study does not establish how Plg activates the 5-LO pathway to induce CD36 expression. Activation of 5-LO can be mediated by p38 mitogen-activated protein kinase activation,[36] and plasmin is known to be a p38 mitogen-activated protein kinase activator.[7] LTB_4 also can activate the intracellular nuclear factors PPARα and weakly PPARγ, but these nuclear factors do not support foam cell formation.[37] Plasmin-induced leukotriene secretion and chemotaxis have been shown to be sensitive to pertussis toxin,[7] which supports our suggestion that LTB_4 signals via binding to BLT_1, a G-protein–coupled receptor. Although our model suggests that released LTB_4 exerts its effects on the expression of CD36 on the same cell, released LTB_4 may stimulate other macrophages or other cells sensitive to LTB_4. LTB_4 but not LTE_4 enhanced CD36 expression, but other products of Plg-induced signaling may exert other far-reaching effects.

Kremen et al[19] demonstrated that Plg deficiency markedly reduced atherosclerosis lesion growth, an observation entirely consistent with our data. In contrast, Xiao et al[18] suggested that Plg deficiency accelerated lesion development. In the Kremen et al study, mice were fed an atherogenic diet; in the Xiao et al study, they were fed a low-fat diet. However, our data showed a diet-independent effect of Plg in macrophage

Downloaded from http://circ.ahajournals.org/ at INSERM U460 UFR XAVIER BI on March 3, 2014

foam cell formation in ApoE$^{-/-}$ mice. In the studies by Xiao et al and Kremen et al, the lesions were observed at different stages of development (15 weeks in the former and 18–25 weeks in the latter study). Plg exerts numerous effects in vivo, and its proatherogenic activities (eg, enhanced ingress of inflammatory cells or enhanced lipid uptake) may dominate its antiatherogenic effects (eg, turnover of extracellular matrix or cytokines) at different stages of lesion development. Such counterbalancing effects of Plg may have contributed to the absence of a significant benefit of tissue-type plasminogen activator therapy on the incidence of mortality and nonfatal myocardial infarction in patients with unstable angina or non–ST-segment–elevation myocardial infarction;[38] the effects of Plg on foam cell formation and accelerated atherosclerosis may have offset the benefits of thrombolysis.

Conclusions

Plg is a key regulator of foam cell formation. Inactivation of Plg reduces OxLDL-driven foam cell formation by reducing the biosynthesis of LTB_4, reducing the expression of CD36, and suppressing OxLDL-driven expression of multiple genes involved in foam cell formation. The combination of these effects identifies a prominent role of Plg in atherogenesis. These findings provide a molecular explanation for the association of Plg with coronary artery disease and provide an impetus to further explore Plg-mediated lipid metabolism and to consider Plg and Plg-Rs as targets for therapeutic intervention in cardiovascular disease.

Acknowledgments

We thank Timothy Burke for technical assistance, Drs Judy Drazba and John Peterson for help with microscopy, and Colin O'Rourke for biostatistical analyses.

Sources of Funding

This work was supported by National Institutes of Health grant HL017964 to Dr Plow and American Heart Association Scientist Development grant 11SDG7390041 to Dr Das.

Disclosures

None.

References

1. Glass CK, Witztum JL. Atherosclerosis: the road ahead. *Cell*. 2001;104:503–516.
2. Shashkin P, Dragulev B, Ley K. Macrophage differentiation to foam cells. *Curr Pharm Des*. 2005;11:3061–3072.
3. Plow EF, Herren T, Redlitz A, Miles LA, Hoover-Plow JL. The cell biology of the plasminogen system. *FASEB J*. 1995;9:939–945.
4. Ploplis VA, Carmeliet P, Vazirzadeh S, Van Vlaenderen I, Moons L, Plow EF, Collen D. Effects of disruption of the plasminogen gene on thrombosis, growth, and health in mice. *Circulation*. 1995;92:2585–2593.
5. Miles LA, Hawley SB, Baik N, Andronicos NM, Castellino FJ, Parmer RJ. Plasminogen receptors: the sine qua non of cell surface plasminogen activation. *Front Biosci*. 2005;10:1754–1762.
6. Plow EF, Hoover-Plow J. The functions of plasminogen in cardiovascular disease. *Trends Cardiovasc Med*. 2004;14:180–186.
7. Syrovets T, Simmet T. Novel aspects and new roles for the serine protease plasmin. *Cell Mol Life Sci*. 2004;61:873–885.
8. Laumonnier Y, Syrovets T, Burysek L, Simmet T. Identification of the annexin A2 heterotetramer as a receptor for the plasmin-induced signaling in human peripheral monocytes. *Blood*. 2006;107:3342–3349.
9. Weide I, Römisch J, Simmet T. Contact activation triggers stimulation of the monocyte 5-lipoxygenase pathway via plasmin. *Blood*. 1994;83:1941–1951.
10. Poeckel D, Funk CD. The 5-lipoxygenase/leukotriene pathway in preclinical models of cardiovascular disease. *Cardiovasc Res*. 2010;86:243–253.
11. Aiello RJ, Bourassa PA, Lindsey S, Weng W, Freeman A, Showell HJ. Leukotriene B4 receptor antagonism reduces monocytic foam cells in mice. *Arterioscler Thromb Vasc Biol*. 2002;22:443–449.
12. Subbarao K, Jala VR, Mathis S, Suttles J, Zacharias W, Ahamed J, Ali H, Tseng MT, Haribabu B. Role of leukotriene B4 receptors in the development of atherosclerosis: potential mechanisms. *Arterioscler Thromb Vasc Biol*. 2004;24:369–375.
13. Rajecki M, Pajunen P, Jousilahti P, Rasi V, Vahtera E, Salomaa V. Hemostatic factors as predictors of stroke and cardiovascular diseases: the FINRISK '92 Hemostasis Study. *Blood Coagul Fibrinolysis*. 2005;16:119–124.
14. Folsom AR, Aleksic N, Park E, Salomaa V, Juneja H, Wu KK. Prospective study of fibrinolytic factors and incident coronary heart disease: the Atherosclerosis Risk in Communities (ARIC) Study. *Arterioscler Thromb Vasc Biol*. 2001;21:611–617.
15. Sakkinen PA, Cushman M, Psaty BM, Rodriguez B, Boineau R, Kuller LH, Tracy RP. Relationship of plasmin generation to cardiovascular disease risk factors in elderly men and women. *Arterioscler Thromb Vasc Biol*. 1999;19:499–504.
16. Morange PE, Bickel C, Nicaud V, Schnabel R, Rupprecht HJ, Peetz D, Lackner KJ, Cambien F, Blankenberg S, Tiret L; AtheroGene Investigators. Haemostatic factors and the risk of cardiovascular death in patients with coronary artery disease: the AtheroGene study. *Arterioscler Thromb Vasc Biol*. 2006;26:2793–2799.
17. Koenig W, Rothenbacher D, Hoffmeister A, Griesshammer M, Brenner H. Plasma fibrin D-dimer levels and risk of stable coronary artery disease: results of a large case-control study. *Arterioscler Thromb Vasc Biol*. 2001;21:1701–1705.
18. Xiao Q, Danton MJ, Witte DP, Kowala MC, Valentine MT, Bugge TH, Degen JL. Plasminogen deficiency accelerates vessel wall disease in mice predisposed to atherosclerosis. *Proc Natl Acad Sci U S A*. 1997;94:10335–10340.
19. Kremen M, Krishnan R, Emery I, Hu JH, Slezicki KI, Wu A, Qian K, Du L, Plawman A, Stempien-Otero A, Dichek DA. Plasminogen mediates the atherogenic effects of macrophage-expressed urokinase and accelerates atherosclerosis in apoE-knockout mice. *Proc Natl Acad Sci U S A*. 2008;105:17109–17114.
20. Iwaki T, Donahue DL, Sandoval-Cooper MJ, Castellino FJ, Ploplis VA. A plasminogen deficiency attenuates atherosclerosis as a result of altered lipoprotein processing [abstract]. Presented at: International Society on Thrombosis and Haemostasis XXII Congress; Boston, Massachusetts; July 11–16, 2009.
21. Iwaki T, Malinverno C, Smith D, Xu Z, Liang Z, Ploplis VA, Castellino FJ. The generation and characterization of mice expressing a plasmin-inactivating active site mutation. *J Thromb Haemost*. 2010;8:2341–2344.
22. Febbraio M, Podrez EA, Smith JD, Hajjar DP, Hazen SL, Hoff HF, Sharma K, Silverstein RL. Targeted disruption of the class B scavenger receptor CD36 protects against atherosclerotic lesion development in mice. *J Clin Invest*. 2000;105:1049–1056.
23. Das R, Burke T, Plow EF. Histone H2B as a functionally important plasminogen receptor on macrophages. *Blood*. 2007;110:3763–3772.
24. Ploplis VA, French EL, Carmeliet P, Collen D, Plow EF. Plasminogen deficiency differentially affects recruitment of inflammatory cell populations in mice. *Blood*. 1998;91:2005–2009.
25. Osterud B, Bjorklid E. Role of monocytes in atherogenesis. *Physiol Rev*. 2003;83:1069–1112.
26. Xie S, Lee YF, Kim E, Chen LM, Ni J, Fang LY, Liu S, Lin SJ, Abe J, Berk B, Ho FM, Chang C. TR4 nuclear receptor functions as a fatty acid sensor to modulate CD36 expression and foam cell formation. *Proc Natl Acad Sci U S A*. 2009;106:13353–13358.
27. Huh HY, Pearce SF, Yesner LM, Schindler JL, Silverstein RL. Regulated expression of CD36 during monocyte-to-macrophage differentiation: potential role of CD36 in foam cell formation. *Blood*. 1996;87:2020–2028.
28. Doi K, Hamasaki Y, Noiri E, Nosaka K, Suzuki T, Toda A, Shimizu T, Fujita T, Nakao A. Role of leukotriene B4 in accelerated hyperlipidaemic renal injury. *Nephrology (Carlton)*. 2011;16:304–309.
29. López-Parra M, Titos E, Horrillo R, Ferré N, González-Périz A, Martínez-Clemente M, Planagumà A, Masferrer J, Arroyo V, Clària J. Regulatory effects of arachidonate 5-lipoxygenase on hepatic microsomal TG transfer protein activity and VLDL-triglyceride and apoB secretion in obese mice. *J Lipid Res*. 2008;49:2513–2523.
30. Xu S, McKeever BM, Wisniewski D, Miller DK, Spencer RH, Chu L, Ujjainwalla F, Yamin TT, Evans JF, Becker JW, Ferguson AD. Expression, purification and crystallization of human 5-lipoxygenase-activating

Downloaded from http://circ.ahajournals.org/ at INSERM U460 UFR XAVIER BI on March 3, 2014

protein with leukotriene-biosynthesis inhibitors. *Acta Crystallogr Sect F Struct Biol Cryst Commun*. 2007;63(pt 12):1054–1057.
31. Park YM, R Kashyap S, A Major J, Silverstein RL. Insulin promotes macrophage foam cell formation: potential implications in diabetes-related atherosclerosis. *Lab Invest*. 2012;92:1171–1180.
32. Halvorsen B, Waehre T, Scholz H, Clausen OP, von der Thüsen JH, Müller F, Heimli H, Tonstad S, Hall C, Frøland SS, Biessen EA, Damås JK, Aukrust P. Interleukin-10 enhances the oxidized LDL-induced foam cell formation of macrophages by antiapoptotic mechanisms. *J Lipid Res*. 2005;46:211–219.
33. Selvarajan S, Lund LR, Takeuchi T, Craik CS, Werb Z. A plasma kallikrein-dependent plasminogen cascade required for adipocyte differentiation. *Nat Cell Biol*. 2001;3:267–275.
34. Hoover-Plow J, Ellis J, Yuen L. In vivo plasminogen deficiency reduces fat accumulation. *Thromb Haemost*. 2002;87:1011–1019.
35. Podrez EA, Febbraio M, Sheibani N, Schmitt D, Silverstein RL, Hajjar DP, Cohen PA, Frazier WA, Hoff HF, Hazen SL. Macrophage scavenger receptor CD36 is the major receptor for LDL modified by monocyte-generated reactive nitrogen species. *J Clin Invest*. 2000;105:1095–1108.
36. Werz O, Klemm J, Samuelsson B, Rådmark O. 5-Lipoxygenase is phosphorylated by p38 kinase-dependent MAPKAP kinases. *Proc Natl Acad Sci U S A*. 2000;97:5261–5266.
37. Li AC, Binder CJ, Gutierrez A, Brown KK, Plotkin CR, Pattison JW, Valledor AF, Davis RA, Willson TM, Witztum JL, Palinski W, Glass CK. Differential inhibition of macrophage foam-cell formation and atherosclerosis in mice by PPARalpha, beta/delta, and gamma. *J Clin Invest*. 2004;114:1564–1576.
38. Anderson HV, Cannon CP, Stone PH, Williams DO, McCabe CH, Knatterud GL, Thompson B, Willerson JT, Braunwald E. One-year results of the Thrombolysis in Myocardial Infarction (TIMI) IIIB clinical trial: a randomized comparison of tissue-type plasminogen activator versus placebo and early invasive versus early conservative strategies in unstable angina and non-Q wave myocardial infarction. *J Am Coll Cardiol*. 1995;26:1643–1650.

CLINICAL PERSPECTIVE

There is an extensive body of literature, including data from large prospective trials, that associates the levels of plasminogen, plasmin:antiplasmin complexes (a reflection of plasminogen activation), and fibrin degradation products (the products of plasmin action) with coronary artery disease, and murine models support the influence of plasminogen deficiency on atherosclerosis. Here, we provide insights into a direct mechanism by which plasminogen influences atherogenesis. In the absence of plasminogen, macrophages, of either human or murine origin, take up substantially less lipid, and their foam cell formation is markedly suppressed. This transformation to foam cells, a hallmark of atherosclerosis, is shown to be dependent on the proteolytic activity generated from plasminogen and on the interaction of plasmin with the macrophage surface. This interaction turns on expression of the gene for CD36; hence, cell-surface expression of CD36, the major receptor for uptake of oxidized phospholipids, is dampened in plasminogen-deficient conditions. The pathway by which plasminogen controls CD36 gene expression is dependent on its activation of 5-lipoxigenase and generation of leukotriene B_4, known effectors of atherogenesis in vivo. Leukotriene B_4 released from plasmin-stimulated macrophages binds to its high-affinity receptor and triggers expression of the CD36 gene. These results identify a basic mechanism by which plasminogen regulates a macrophage function that is an essential component of atherogenesis, provides an explanation for the association of plasminogen with cardiovascular disease, and may open up new approaches to consider in the treatment of atherosclerosis.

Downloaded from http://circ.ahajournals.org/ at INSERM U460 UFR XAVIER BI on March 3, 2014

Correction

In the article by Das et al, "Macrophage Gene Expression and Foam Cell Formation Are Regulated by Plasminogen," which was published in the March 19, 2013 issue of the journal (*Circulation*. 2013;127:1209–1218), a correction is needed.

In Figure 5B on page 1213, the second set of bars should be labeled as FcγRII instead of FcγR1 and the third set as FcγR1 instead of FcγRII. Accordingly the text on page 1213, "Among other genes, OxLDL-mediated CD68 (Figure 5A), Fcγ receptor type 1,…", should read: "Among other genes, OxLDL-mediated CD68 (Figure 5A), Fcγ receptor type II,…".

The current online version of the article has been corrected. The authors regret the error.

(*Circulation*. 2014;129:e326.)
© 2014 American Heart Association, Inc.
***Circulation* is available at http://circ.ahajournals.org** **DOI: 10.1161/CIR.0000000000000011**

Supplementary materials

Supplemental Material and Methods:

Ex vivo foam cell formation

Plg+/+ and Plg-/- mice were injected i.p. with 0.5 ml of 4% TG and blood (via inferior vena cava) and peritoneal cells (90% macrophages) were collected after 3 days. Serum was obtained by incubating the collected blood at 22˚C for 15 min followed by centrifugation. Isolated peritoneal macrophages were incubated with 200 μM TXA followed by three washes with PBS. This step was performed to remove surface bound Plg from the macrophages and did not affect cell viability as assessed by trypan blue exclusion. Cells were plated onto 8-well chamber slides (Lab-Tek) or 12-well plates (Corning) in RPMI 1640. After 2 h, non-adherent cells were removed, and fresh medium with 10% serum derived from Plg+/+ or Plg-/- mice was added for 24 hr. Cells were then incubated with 50 μg/ml OxLDL (Biomedical Technologies, Inc, Stoughton, MA) for 24-48 hr in the presence or absence of various inhibitors. Throughout the course of these studies, similar results were obtained with at least 7 different lots of OxLDL. Cells in the 8-well chamber slides were fixed with 4% paraformaldehyde, stained with Oil-Red-O (ORO, Sigma), counterstained with hematoxylin QS (Vector laboratories) and mounted in VectaMount AQ (Vector Laboratories) for microscopic examination. Cells in 12-well plates were used to extract lipids and proteins as described previously[1]. Briefly, total lipids were extracted from cells by adding hexane: isopropanol at a 3:2 ratio. The solvent was collected to measure total cholesterol using the Cholesterol/Cholesteryl Ester Quantification Kit II from Biovision, Milpitas; CA. Proteins were extracted from the

cells using 0.1 M NaOH and quantified by the Bradford method (BioRad). Values of total cholesterol were normalized to the total protein content of extracts.

In vivo foam cell formation

ApoE-/- or ApoE-/-Plg-/- mice, fed either CD or HCD, were injected i.p. with TG and peritoneal cells were collected after 3 days and allowed to adhere for 30 min in the 8-well chamber slides or 12-well plates. After removing non-adherent cells, the adherent macrophages were either stained with ORO or extracted to measure total cholesterol.

In vivo transfer of macrophages

This experiment was performed as described previously[2]. TG-elicited peritoneal macrophages were isolated from male Plg+/+ donor mice and washed with TXA. A total of 12 $x10^6$ live cells were then injected i.p. into recipient male ApoE-/- or ApoE-/-Plg-/- mice, which had been maintained on either chow or HC diet for 6 weeks [2]. After 3 days, peritoneal macrophages were collected and assessed for ORO staining and total cholesterol as described above.

Foam cell formation in THP-1 and in human peripheral blood monocytes

THP-1 cells were obtained from ATCC and cultured as described before[3]. For foam cell formation assay, THP-1 cells were cultured in fibronectin-coated plastic wells (Calbiochem) and treated with 15 nM PMA on for 24 h in complete media. Cells were then washed and treated with OxLDL (50 μg/ml) for an additional 48 hr in either 10% FBS or 10% FBS depleted of Plg in theTHP-1 medium. Cells were analyzed for foam

cell formation by either staining with Oil Red O or quantifying total cholesterol as described above.

To obtain HuPBM, peripheral blood was obtained from healthy donors using an informed consent form approved by Institutional Review Board of Cleveland Clinic. A portion of the blood was used to purify serum while the other portion was used to isolate monocytes. Monocytes were isolated using Ficol Hypaque (Amersham) followed by adherence to fibronectin coated plates (BD Bioscience). The adherent monocytes were cultured for 48 h in RPMI-1640 in either 10% autologous serum or Plg-depleted 10% autologous serum to obtain human peripheral blood derived macrophages. Cells were then treated with 50 μg/ml OxLDL for 24 h in presence of the autologous serum or autologous serum depleted of Plg. Peripheral blood was collected from three different donors and performed foam cell formation experiment independently.

RAW264.7 cells culture and treatment.

RAW264.7 cells were obtained from ATCC and cultured in DMEM containing 10% fetal bovine serum, 4 mM L-glutamine, 1.5 g/L sodium bicarbonate, 4.5 g/L glucose and 1 mM sodium pyruvate. For experimental studies, the RAW264.7 cells were transferred to 1% Nutridoma-SP (Roche, Germany) in DMEM and cultured for 2 h. Cells were washed, added to fresh 1% Nutridoma medium and treated with either Glu-Plg (Enzyme Research, South Bend, IN) or MK-886, Ly39111, U75302 (Cayman, Ann Arbor, MI) and then treated with Plg for 24 h.

Real time RT-PCR

Total RNA was extracted from macrophages using RNeasy minikits (Qiagen) followed by digestion of genomic DNA using RNase free DNase 1 (Fermentas). A total of 1 μg RNA was transcribed into cDNA using iScript reverse transcriptase (BioRad) and a mixture of oligo (dT) and random primers in a total volume of 25 μl. Reverse transcribed RNA was primed with oligonucleotides specific for each of the genes (supplemental Table 1) to be analyzed. Quantitative PCR was performed in a 20 μl reaction volume containing 2 μl of a 10-fold diluted cDNA, 10 μl 2X SYBER Green PCR master mix (BioRad) and 0.5 pmol sense or antisense primers. The qPCR reactions were performed on optical 96-well strips with optical caps in the BioRad iCycler PCR system (Model: MyiQ2, BioRad). The same thermal profile conditions were used for all primers sets: 50^{o}C for 2 minutes, 95^{o}C for 10 minutes, and then 40 cycles of 95^{o}C for 15 seconds and 60^{o}C for 1 minute. All samples were analyzed in triplicate, and cyclophilin A content was used for normalization as previously described[4].

Western blots

Cells were disrupted in lysis buffer consisting of 50 mM Tris-HCl, pH 7.5, 150 mM NaCl, 1% Nonidet P-40, 0.5% sodium deoxycholate and a protease inhibitor cocktail tablet (Roche Diagnostics, Indianapolis, IN). Lysates were analyzed by SDS-PAGE on 10% gels and electrophoretically transferred to nitrocellulose membranes (Bio-Rad, Hercules, CA). The membranes were blocked with 5% BSA in TBS-T (Tris borate saline containing 0.1% Tween-20), probed with rat anti-mouse-CD36 (R&D) or rabbit anti-mouse CD36 (Novus Biologicals) followed by HRP-anti-rat or HRP- anti-rabbit

(Calbiochem) and subsequently developed with ECL detection kits (Santa Cruz Biotechnology, Inc, Santa Cruz, CA). The intensities of Western blot bands were measured by using Kodak ID 3.6 software, assigning the intensity of each band of interest in the unstimulated cells a value of 1.0; and the fold change of a particular protein was calculated relative to the corresponding control band.

Flow Cytometry

Cells were detached from plastic wells using enzyme-free dissociation buffer (Invitrogen), washed and Fc receptors blocked with seroblocker (AbD Serotec, Raleigh, NC). The extent of cell surface CD36 expression was measured by incubating cells with FITC-labeled rat anti-mouse CD36 antibodies (Cayman, Ann Arbor, MI). Cell fluorescence was measured using instruments from BD Bioscience (Bedford, MA) and Cell Quest software.

OxLDL binding and internalization

Macrophage binding and internalization of OxLDL were performed using OxLDL labeled with fluorescent probe, 1,1'-dioctadecyl-1 to 3,3,3',3'-tetramethylindocarbocyanine perchlorate (Dil, Biomedical Technologies, inc) as described previously[5]. After specified culture conditions, cells were extensively washed and incubated with different concentration of Dil-OxLDL in DMEM containing 2% lipoprotein-deficient human serum in absence or presence of 20 fold excess OxLDL. The extent of binding, measured after 30 min at 4^{o}C or internalization, measured after 2 hr at 37 ^{o}C was determined by flow cytometry. Specific mean fluorescence intensity (MFI)

values were obtained by subtracting the MFI of Dil-OxLDL + Excess OxLDL from MFI of Dil-OxLDL alone. The resulting specific binding values were used to construct ligand binding and internalization curves.

Serum LTB4 measurement

Serum was isolated from blood as described above and stored at -70^{o}C until assay. LTB4 levels in serum were quantified using a kit from Cayman Chemical, Ann Arbor, MI, according to manufacturer's protocol. The assay is based on a competition between the serum LTB4 and an LTB4-acetylcholineesterase conjugate for a limited amount of LTB4 antiserum coated on plastic wells.

LTB4, Plg and LDL/VLDL measurement.

These components were measured in 1.5 ml of 1X PBS used to lavage the peritoneal cavity of TG stimulated ApoE-/- and ApoE-/-Plg-/- mice fed with either CD or HFD. LTB4 levels in peritoneal fluid were measured using LTB4 measurement kits which are based on a competition between the serum LTB4 and an LTB4-acetylcholineesterase conjugate for a limited amount of LTB4 antiserum coated onto plastic wells. LDL/VLDL levels in peritoneal fluid were measured using a quantification kit from Biovision, Milpitas, CA. Plg levels in peritoneal wash was quantified by using an ELISA kit designed for detecting mouse Plg (American Diagnostica, GmbH).

Preparation of plasminogen-depleted fetal bovine serum

FBS was recycled three times through a lysine-Sepharose 4B column (GE Healthcare, Piscataway, NJ) and flow-through from the third pass was collected. A >70% depletion of Plg in flow-through serum was confirmed based on plasmin activity as measured using the S2251 chromogenic substrate S2251 and LMW uPA[6].

Statistical Analysis

A two-tailed *t* test was used in comparing two groups, and differences between multiple groups were evaluated using either a one-way ANOVA or a two-way ANOVA test followed by Tukey multiple comparison test. Normality of data was tested using Shapiro-Wilk test. These statistical analyses were performed using either SigmaPlot 12 software or R software (version 2.15.1, Vienna, Austria). Values are expressed as means ± SD, and p values of ≤0.05 were considered significant. Analysis for Figures 1[B], 6[B] and 7[B] were performed using two tailed t-tests. Analysis for Figure 1[D], 1[E], 2[B], 2[D], 3[E], 6[D], 7[D], 7[E], 7[F] and supplemental Figure S2&S3 were performed using a one-way ANOVA followed by Tukey multiple comparison test. Analysis for Figures 3[A]-3[D], 4[B] and 4[D] were performed using a two-way ANOVA followed by Tukey multiple comparison tests. All these analyses were performed using SigmaPlot version 12. Analysis for Figure 6[E] was performed with a combination of one-way and two-way ANOVA followed by Tukey multiple comparison tests. Figure 7[B] and Figure S4 were analyzed by one-way ANOVA followed by Tukey multiple comparison tests. All these analysis were performed using R software version 2.15.1.

Supplemental Tables

Supplemental Table 1. Primers

Gene	Forward primer (5' to 3')	Reverse primer (5' to 3')
CD36	CAGCAAGGCCAGATATCACA	TGCAGCTGAGCAGAAAGAGA
LDLR	GAAAAGGCTACTGGCTGTGC	CCAGGACCCGGTCAGTAGTA
ABCA1	TTGTTCCAAAGAGCCATGTG	GCTTGGAATGAGGGCCAATG
CD68	AGGGTGGAAGAAAGGTAAAGC	AGAGCAGGTCAAGGTGAACAG
MSR-A	ATGATCGCTGGGATATACGG	ACCCCAGCATCTTCTGAATG
PSR1	TCTGCTCAATGCACAAGAGG	TGGGCACCTTGTAGTCTTCC
PPAR-γ	ACATAAAGTCCTTCCCGCTGACCA	AAATTCGGATGGCCACCTCTTTGC
CEBP α	AAACAACGCAACGTGGAGA	GCGGTCATTGTCACTGGTC
CEBP β	TGATGCAATCCGGATCAA	CACGTGTGTTGCGTCAGTC
FcγRI	GCAAGTTAGAAGCGATGGCG	TGGGGGTATCTGGACCTGAG
FcγRII	GGAAGGGGAAACCATCACG	CAGAGGGCTGTCTGTACTC
SRB1	CAGTAGTTCTGCCGTTGCTG	TGAATGGCCTCCTTATCCTG
TR4	CAGCCATTGTCAACCACCTA	TTGCTTTATCCGGTCACCA
Cyclophilin	TGGAGAGCACCAAGACAGACA	TGCCGGAGTCGACAATGAT

Supplemental Table 2: Plasma Cholesterol levels

Genotype	Weight (gm)		LDL/VLDL (mg/dl)		HDL (mg/dl)	
	CD	HCD	CD	HCD	CD	HCD
ApoE-/-	25-30	30-32	259.4 (±20)	1085 (±146)	52.6 (±6.5)	40.3 (±6)
ApoE-/-Plg-/-	22-27	24-27	346.2 (±78)	832.3 (±113)	20.7* (±6)	27.5 (±3)*

Values are expressed as mean ± SD, n=5.

*p<0.01 vs. ApoE-/-.

Supplemental Figure legends.

Figure S1. ORO staining to detect formation of foam-like cells by THP-1 (panel A, at original 20X magnification) and RAW 264.7 cells (panel B, at original 20X magnification) **(A)** Depletion of Plg from fetal bovine serum (FBS) impairs OxLDL mediated foam cell formation by differentiated (PMA, 15 nM) THP-1 cells. Addition of exogenous Plg (1 μM) restores the foam cell phenotype associated with Plg depletion. **(B)** Plg (0.5 to 1 μM) induces OxLDL mediated foam cells by RAW264.7 cells cultured in 1 % Nutridoma (Roche) in DMEM for 24 hr.

Figure S2. Plasminogen regulates CD36 expression by activating 5-LO pathway.

Panels A&B: Western blot analysis for CD36 protein (upper panels in RAW264.7 cells treated with either Plg or with the 5-LO inhibitor, MK886, and treated with Plg (1 μM) in DMEM supplemented with 1% Nutridoma. Some cells were treated with LTB4 (500 nM) or with Plg + LTB4. Western blot of actin was used as a loading control (lower panels in A&B). Each dot in lower panels of A&B is one of three replicate fold values. Fold values are derived from 3 sets of blots from 3 independent experiments. Error bars are the SD of the means. In panel A CD36 protein was detected by an antibody obtained from R&D. In this panel, bands lower than expected molecular weight of CD36 show the similar pattern of changes as CD36 bands.

CD36 protein in panel B was detected by an antibody derived from Novus Biologicals.

Figure S3. Plg mediated CD36 expression is regulated via LTB4 receptor, BLT1. Western blot analysis for CD36 protein (upper panels) in RAW264.7 cells treated either with Plg or with the BLT1 blockers, Ly39111 or U75302 (Cayman Chemicals) and then treated with Plg (1 μM) in DMEM supplemented with 1% Nutridoma. Western blot of actin was used as a loading control. CD36 was detected by an antibody derived from Novus Biologicals. Each dot in lower panel is one of three replicate fold values. Fold values are derived from 3 sets of blots from 3 independent experiments. Error bars are the SD of the means.

Figure S4. Plg mediated CD36 expression is mediated by LTB4 but not LTE4. Western blot analysis for CD36 protein in RAW264.7 cells treated with Plg (1 μM), LTB4, or LTE4 in DMEM supplemented with 1% Nutridoma. Actin was used as a loading control in the Western blots. Data are representative of 3 independent experiments. CD36 was detected by an antibody derived from Novus Biologicals. Each dot in lower panels of A&B is one of three replicate fold values. Fold values are derived from 3 sets of blots from 3 independent experiments. Error bars are the SD of the means.

Supplemental Reference List

(1) Robinet P, Wang Z, Hazen SL, Smith JD. A simple and sensitive enzymatic method for cholesterol quantification in macrophages and foam cells. *J Lipid Res.* 2010;51:3364-3369.

(2) Rahaman SO, Lennon DJ, Febbraio M, Podrez EA, Hazen SL, Silverstein RL. A CD36-dependent signaling cascade is necessary for macrophage foam cell formation. *Cell Metab.* 2006;4:211-221.

(3) Das R, Burke T, Van Wagoner DR, Plow EF. L-type calcium channel blockers exert an antiinflammatory effect by suppressing expression of plasminogen receptors on macrophages. *Circ Res.* 2009;105:167-175.

(4) Szatmari I, Pap A, Ruhl R et al. PPARgamma controls CD1d expression by turning on retinoic acid synthesis in developing human dendritic cells. *J Exp Med.* 2006;203:2351-2362.

(5) Ouchi N, Kihara S, Arita Y, Nishida M, Matsuyama A, Okamoto Y, Ishigami M, Kuriyama H, Kishida K, Nishizawa H, Hotta K, Muraguchi M, Ohmoto Y, Yamashita S, Funahashi T, Matsuzawa Y. Adipocyte-derived plasma protein, adiponectin, suppresses lipid accumulation and class A scavenger receptor expression in human monocyte-derived macrophages. *Circulation.* 2001;103:1057-1063.

(6) Das R, Burke T, Plow EF. Histone H2B as a functionally important plasminogen receptor on macrophages. *Blood.* 2007;110:3763-3772.

[A]

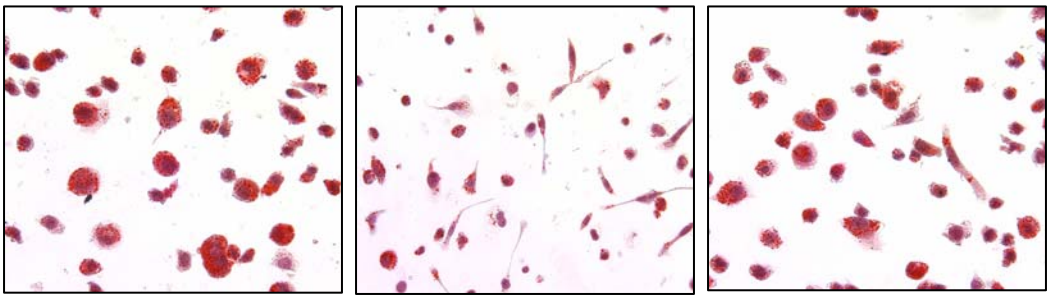

FBS + OxLDL

Plg- depleted FBS + OxLDL

Plg-depleted FBS + Glu-Plg + OxLDL

[B]

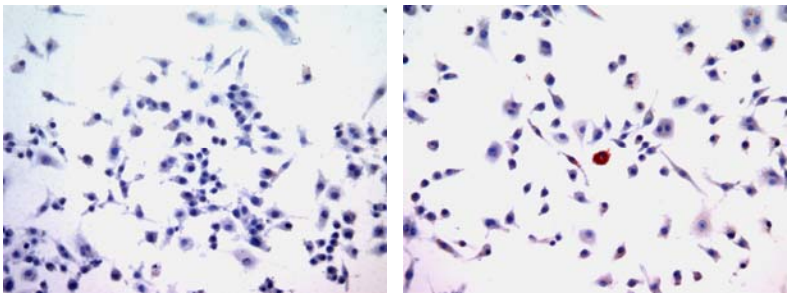

No OxLDL

OxLDL

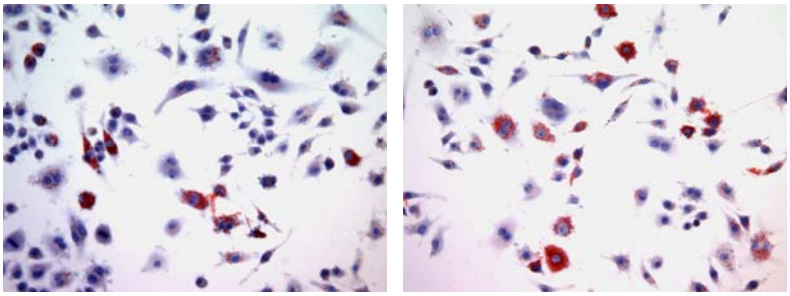

OxLDL + 0.5 μM Plg

OxLDL + 1 μM Plg

Figure S1

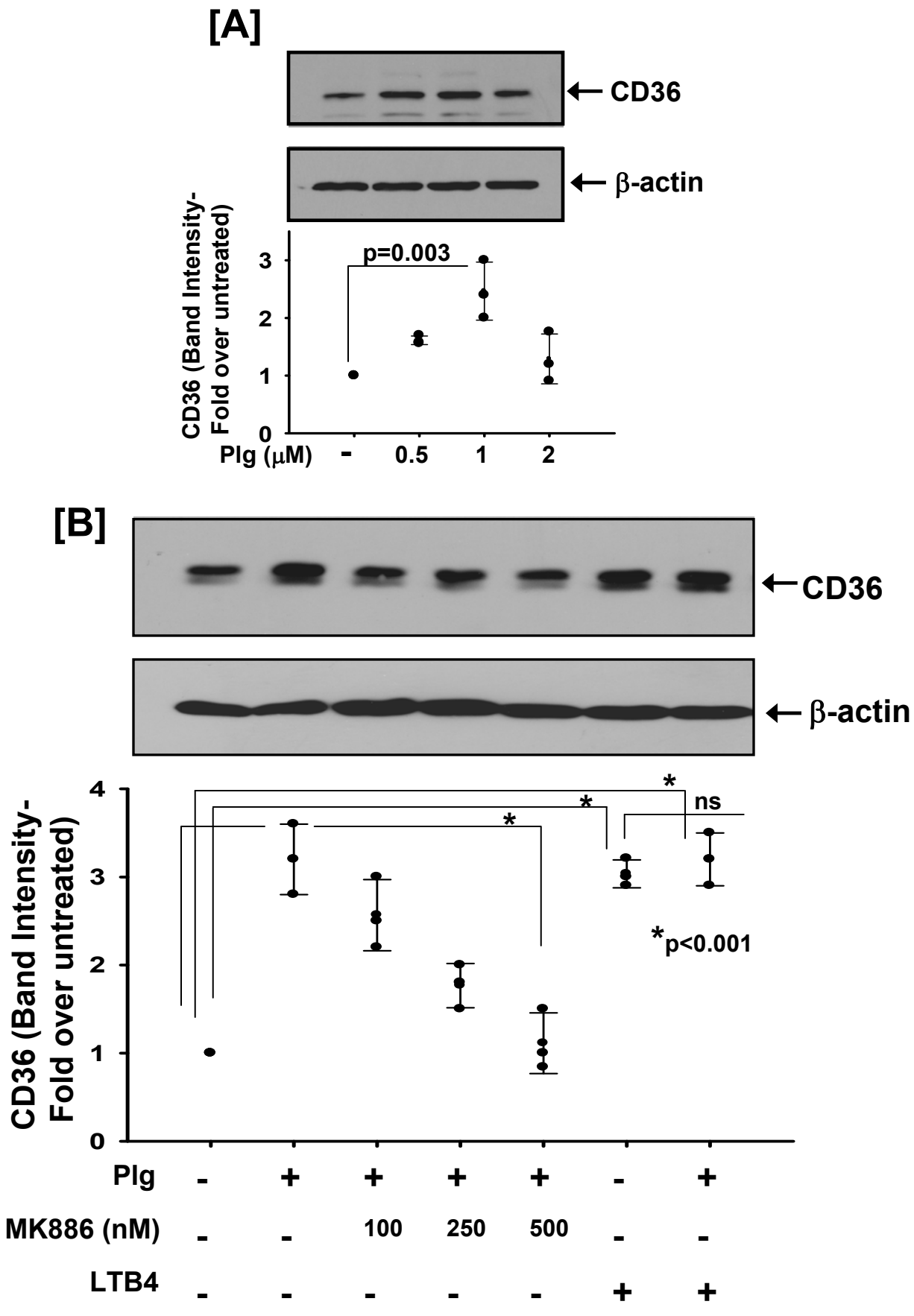

Figure S2 CIRCULATIONAHA/2012/121871 (Supplem.): R14

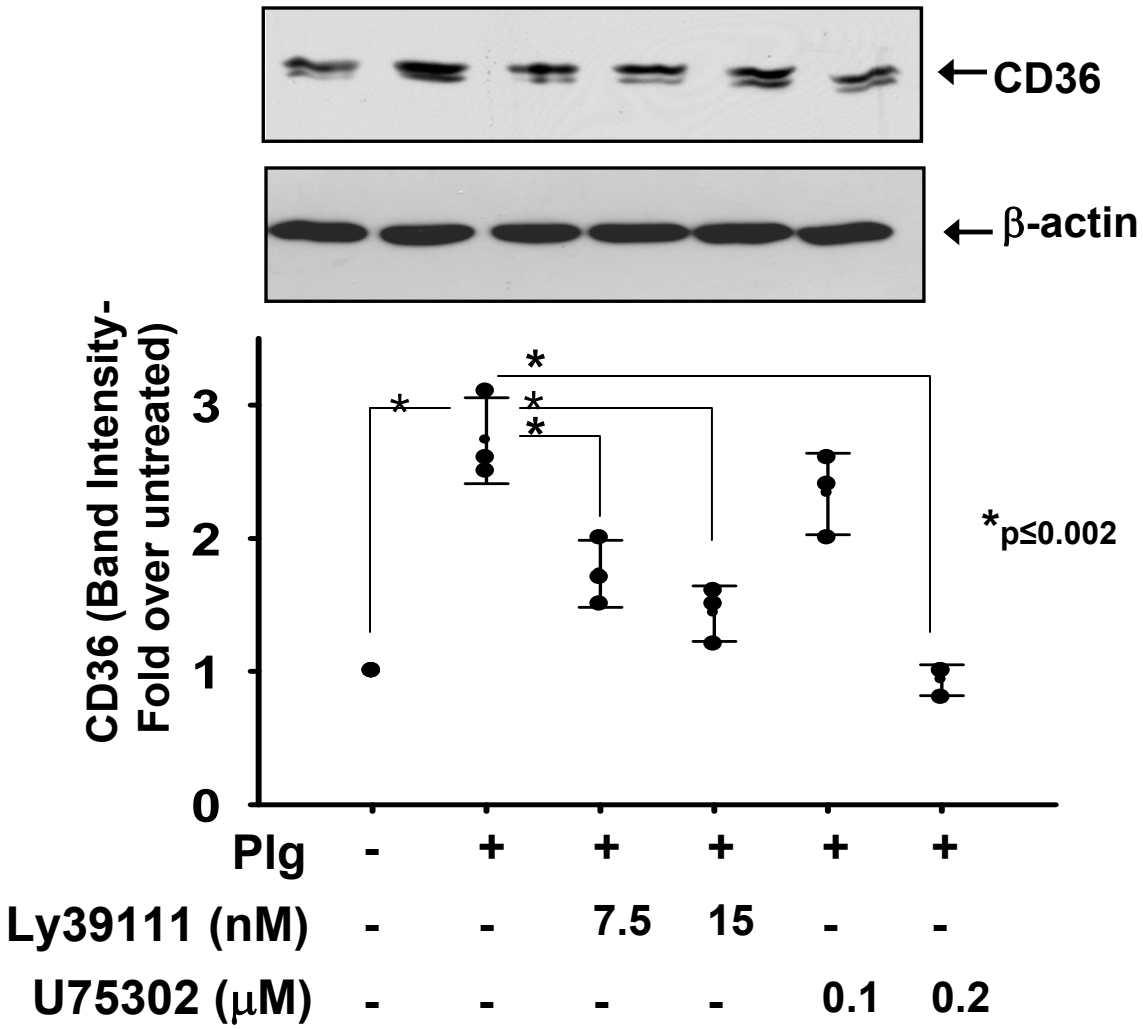
CD36
β-actin
CD36 (Band Intensity-
Fold over untreated)
0
1
2
3
*
*
*
*
*p≤0.002
Plg - + + + + +
Ly39111 (nM) - - 7.5 15 - -
U75302 (μM) - - - - 0.1 0.2

Figure S3

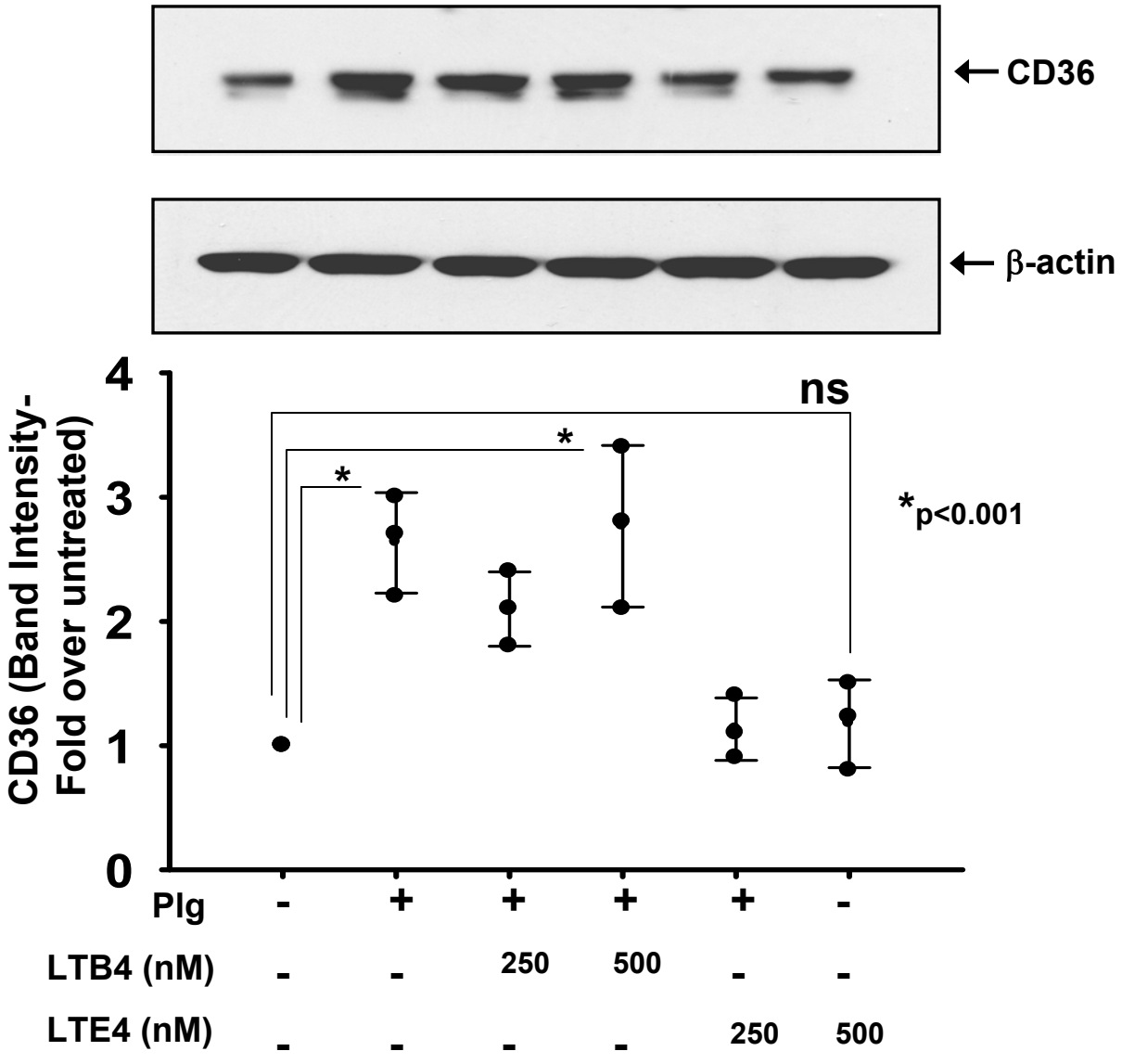
CD36
β-actin
CD36 (Band Intensity-Fold over untreated)
4
3
2
1
0
ns
*
*
*p<0.001
Plg
LTB4 (nM)
LTE4 (nM)
- + + + + -
- - 250 500 - -
- - - - 250 500

Figure S4